

# Passive Stiffness Changes Due To Upregulation of Compliant Titin Isoforms in Human Dilated Cardiomyopathy Hearts

I. Makarenko,\* C.A. Opitz,\* M.C. Leake, C. Neagoe, M. Kulke, J.K. Gwathmey, F. del Monte, R.J. Hajjar, W.A. Linke

**Abstract**—In the pathogenesis of dilated cardiomyopathy, cytoskeletal proteins play an important role. In this study, we analyzed titin expression in left ventricles of 19 control human donors and 9 severely diseased (nonischemic) dilated cardiomyopathy (DCM) transplant-patients, using gel-electrophoresis, immunoblotting, and quantitative RT-PCR. Both human-heart groups coexpressed smaller ( $\approx 3$  MDa) N2B-isoform and longer (3.20 to 3.35 MDa) N2BA-isoforms, but the average N2BA:N2B-protein ratio was shifted from  $\approx 30:70$  in controls to 42:58 in DCM hearts, due mainly to increased expression of N2BA-isoforms  $>3.30$  MDa. Titin per unit tissue was decreased in some DCM hearts. The titin-binding protein obscurin also underwent isoform-shifting in DCM. Quantitative RT-PCR revealed a 47% reduction in total-titin mRNA levels in DCM compared with control hearts, but no differences in N2B, all-N2BA, and individual-N2BA transcripts. The reduction in total-titin transcripts followed from a decreased area occupied by myocytes and increased connective tissue in DCM hearts, as detected by histological analysis. Force measurements on isolated cardiomyofibrils showed that titin-based passive tension was reduced on average by 25% to 30% in DCM, a reduction readily predictable with a model of wormlike-chain titin elasticity. Passive-tension measurements on human-heart fiber bundles, before and after titin proteolysis, revealed a much-reduced relative contribution of titin to total passive stiffness in DCM. Results suggested that the titin-isoform shift in DCM depresses the proportion of titin-based stiffness by  $\approx 10\%$ . We conclude that a lower-than-normal proportion of titin-based stiffness in end-stage failing hearts results partly from loss of titin and increased fibrosis, partly from titin-isoform shift. The titin-isoform shift may be beneficial for myocardial diastolic function, but could impair the contractile performance in systole. (*Circ Res.* 2004;95:000-000.)

**Key Words:** connectin ■ heart-failure ■ diastole/dilated-cardiomyopathy ■ passive-tension

Dilated cardiomyopathy (DCM) is a frequent heart disease, the triggers of which are multifaceted and include gene mutations, as well as environmental factors.<sup>1</sup> A general feature of DCM is the occurrence of myocardial remodeling involving proteins of the cytoskeleton and the extracellular matrix (ECM).<sup>1-4</sup> Alterations in cytoskeletal protein expression, increased fibrosis, and degeneration of hypertrophied myocytes all are associated with chronic heart failure attributable to end-stage human DCM.<sup>3,5</sup> Familial forms of human DCM are characterized by mutations predominantly in those myocardial proteins involved in force transmission.<sup>1,4</sup> Among them is titin, a giant elastic protein of the myofibrillar cytoskeleton.<sup>6-8</sup>

Titin molecules span half-sarcomeres and are essential for myofibrillar assembly.<sup>9</sup> Titin's I-band part contributes substantially to passive-tension (PT) development<sup>10-12</sup> and short-

ening velocity.<sup>13</sup> The reported DCM-causing mutations in titin localize to the molecule's Z-disk region<sup>6</sup> or elastic I-band segment<sup>7,8</sup> and are expected to impair the mechanical function of titin leading to stress-sensing defects.<sup>14</sup> Furthermore, electron-microscopical and immunocytochemical studies on human end-stage failing DCM hearts showed altered distribution and loss of titin.<sup>2</sup> Loss of cross-striations and decreased expression of titin was also evident in failing hearts of hamsters<sup>15</sup> and guinea pigs.<sup>16,17</sup> Such titin changes are likely to affect myocardial PT-development and/or force transmission in pathological states of the heart.

Human-cardiac titin is expressed in two main isoforms, N2B (3000 kDa) and N2BA (3200 to 3350 kDa).<sup>18</sup> The different-length isoforms result from alternative splicing of titin's elastic I-band region (Figure 1A). Recently, we reported a change in the N2BA:N2B ratio of human cardiac

Original received July 30, 2003; resubmission received July 20, 2004; revised resubmission received August 17, 2004; accepted August 23, 2004.

From the Physiology and Biophysics Laboratory (I.M., W.A.L.), University of Muenster, Muenster, Germany; Institute of Physiology (C.A.O., M.C.L., C.N., M.K., W.A.L.), University of Heidelberg, Heidelberg, Germany; Boston University Medical Center (J.K.G.), Boston, Mass; and the Cardiovascular Research Center (F.d.M., R.J.H.), Massachusetts General Hospital, Boston, Mass.

\*Both authors contributed equally to this study.

Correspondence to Wolfgang A. Linke, PhD, Physiology and Biophysics Laboratory, University of Muenster, Schlossplatz 5, D48149 Muenster, Germany. E-mail wlinke@uni-muenster.de

© 2004 American Heart Association, Inc.

*Circulation Research* is available at <http://www.circresaha.org>

DOI: 10.1161/01.RES.0000143901.37063.2f

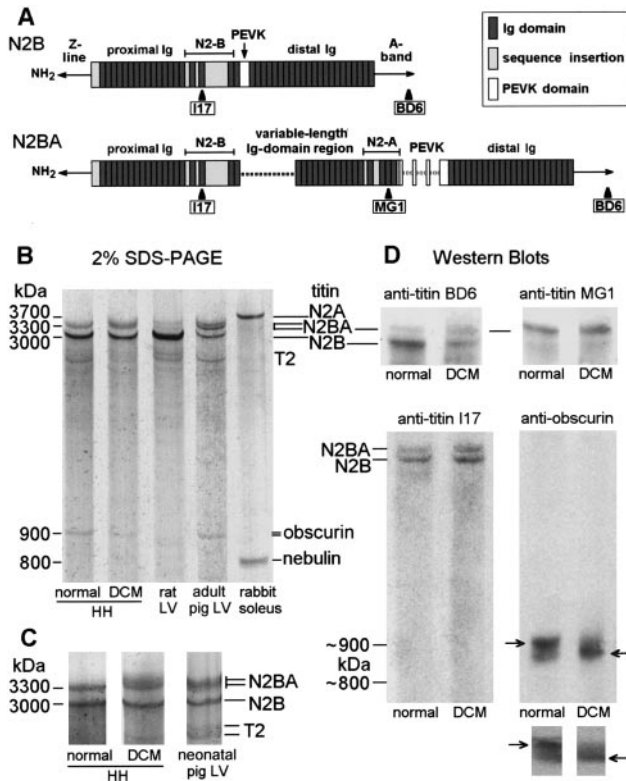


**Figure 1.** Titin-isoform expression in human heart analyzed by 2% SDS-PAGE and Immunoblotting. A, Domain structure of elastic I-band-titin isoforms in HH. Positions of titin-antibodies used are indicated (boxes). B, Comparison of titin-expression pattern in normal-human and DCM LV with that in rat and pig adult LV and rabbit soleus (N2A=3700 kDa). T2 indicates titin-degradation band. Coomassie-staining. C, Titin-isoforms in normal, DCM, and neonatal pig LV, silver-staining. D, Immunoblotting using antibodies to titin and obscurin (arrows).

titin, from  $\approx 30:70$  in normal heart to nearly 50:50 in chronically ischemic myocardium of coronary artery disease (CAD) patients, thereby lowering titin-derived PT.<sup>19</sup> A canine model of pacing-induced DCM showed a change in the transmural isoform-ratio gradient in hearts paced for two weeks, compared with controls, without a change in the average ratio.<sup>20</sup> However, the average N2BA:N2B ratio changed significantly from  $\approx 50:50$  in normal dog hearts to

44:56 after four weeks of pacing.<sup>21</sup> These studies<sup>10,21</sup> established that a titin-isoform shift occurs in pathological situations of cardiac overload.

In this work, we report that failing human (nonischemic) DCM hearts express increased N2BA:N2B titin-protein ratios over control donor hearts, whereas no change in N2BA:N2B ratio occurs at the mRNA level. Thus, the upregulation of compliant titin-isoforms in DCM is likely to be regulated downstream of alternative splicing. However, the total-titin mRNA-transcripts were reduced by nearly half in DCM, most likely attributable to loss of cardiomyocytes, as suggested by histological evidence. In force measurements on isolated myofibrils, the protein-isoform shift in DCM caused reduced titin-based passive stiffness. Fiber-bundle mechanics showed that the relative contribution of titin to total passive stiffness is reduced in DCM, and part of this effect is ascribable to titin-isoform switching. The switch toward more compliant titin-isoforms may help the surviving myocytes in end-stage failing DCM tissue to partially counteract an increased global stiffness mainly caused by fibrosis.

## Materials and Methods

### Human-Heart Tissue

Left-ventricular (LV) samples obtained from human hearts (HH) were classified into two groups, control ("normal") donors (n=19; set1=10, set2=9), and transplant-HHs diagnosed with severe nonischemic DCM (n=9; Table). Tissue handling and tests for tissue preservation are detailed in the expanded Materials and Methods in the online data supplement available at <http://circres.ahajournals.org>. Procedures were performed in accordance with institutional guidelines.

### High-Resolution Gel-Electrophoresis and Immunoblotting

Agarose-strengthened 2% SDS-polyacrylamide gels were optimized to detect the MDA-size titin-isoforms.<sup>19</sup> Unless indicated otherwise, gels were stained with Coomassie brilliant-blue. Gel-densitometry was performed as described.<sup>19</sup> Immunoblotting was done with a chemiluminescent reaction kit (ECL-system, Amersham-Pharmacia) according to standard protocols. For antibodies against titin and obscurin, see Figure 1A and online data supplement.

### Quantitative RT-PCR

Real-time qRT-PCR was performed as described<sup>22</sup> using an ABI-7000 thermal cycler and SYBR-Green PCR-Mastermix (Applied Biosystems). For details and primers, see online data supplement.

### Hemodynamic Parameters for End-Stage Failing Human-DCM Hearts

| HH No. | Etiology<br>(Time Period, y, Since<br>Diagnosis of Disease) | NYHA Class | LV End-Diastolic<br>Inner Diameter,<br>mm* | Pulmonary Artery<br>Pressure,<br>mm Hg | Cardiac index,<br>L/min/m <sup>2</sup> | Pulmonary capillary<br>wedge pressure,<br>mm Hg | Ejection<br>Fraction |
|--------|---|------------|--|--|--|---|----------------------|
| 1      | DCM(1.5)  | 4          | 68   | 68/31                                  | 1.9                                    | 45  | 10                   |
| 2      | DCM(3.0)  | 4          | 61   | 30/14                                  | 1.9                                    | 14  | 21                   |
| 3      | DCM(4.3)  | 4          | 60   | 45/20                                  | 1.9                                    | 28  | 18                   |
| 4      | DCM(0.8)  | 4          | 62   | 48/30                                  | 1.7                                    | 22  | 30                   |
| 5      | DCM(3.8)  | 4          | 70   | 56/21                                  | 2.1                                    | 24  | 20                   |
| 6      | DCM(2.1)  | 4          | 60   | 34/12                                  | 2.6                                    | 17  | 22                   |
| 7      | DCM(3.3)  | 4          | 65   | 46/26                                  | 2.2                                    | 19  | 19                   |
| 8      | DCM(5.2)  | 4          | 58   | 41/18                                  | 2.0                                    | 24  | 16                   |
| 9      | DCM(3.1)  | 4          | 63   | 42/20                                  | 1.8                                    | 25  | 17                   |

\*Normal values, 37 to 53 mm.

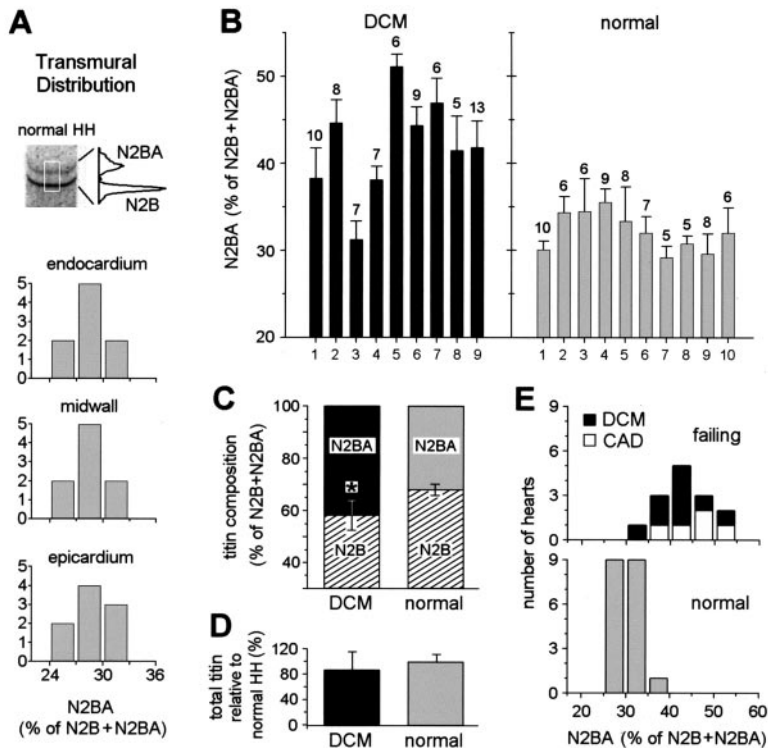


**Figure 2.** Titin-isoform composition in normal and failing HHs. A, Histograms showing distribution of N2BA-titin content across the free LV wall of 9 normal-donor hearts. B, Relative N2BA-titin content (means for individual hearts); the number of gel-lanes analyzed per HH-sample is indicated. C, Mean titin-isoform composition of both HH-groups. \* $P < 0.001$  in Student  $t$  test. D, Total-titin content per unit tissue, shown as DCM relative to normal-HH average. E, Histogram distribution of the proportion of N2BA-titin. DCM data are from B, CAD-data from Neagoe et al.<sup>19</sup> Normal-HH data are from A, midwall, and B. Data in B through D are mean  $\pm$  SD.

## Histology

HH-sections were stained with Fuchsin acid and Aniline-blue/Orange-G (Mallory staining). Slides were viewed and images recorded using a Leitz-Orthomat-W microscope. Analysis of myocyte area was done with ScionImage.

## Myofibril Mechanics

Cardiac myofibrils were prepared<sup>19,23</sup> from frozen HH-tissue (4 DCM HHs, 4 control-donors). Under a Zeiss-Axiovert-135 microscope, myofibrils were suspended between glass needles attached to a piezoelectric actuator (Physik-Instrumente) and a force-transducer (homebuilt) with nanonewton resolution.<sup>19,23</sup> For experimental protocols, see expanded Materials and Methods.

## Fiber Mechanics

Fiber bundles 400 to 500  $\mu$ m in diameter were dissected from three normal and three DCM human LV and skinned in Triton-X-100 overnight. Using a workstation for muscle mechanics (Scientific Instruments),<sup>13,19</sup> stretch-release loops were performed and passive force was measured before and after degradation of titin by low doses of trypsin, following a protocol described elsewhere.<sup>24</sup>

## Modeling

Myofibrillar PT was modeled (see expanded Materials and Methods) using a force-extension curve generated from the weighted sum of three wormlike-chain force-extension relations corresponding to the different extensible regions in cardiac titin.<sup>11</sup>

## Results

### Titin-Protein Expression in Normal and DCM Human Heart

2% SDS-PAGE (Figure 1B and 1C) was performed to detect the cardiac-titin isoforms, N2B and N2BA (Figure 1A), in 10 control-donor HHs (set1) and 9 end-stage failing hearts explanted from severely diseased DCM patients (Table). Titin expression was also analyzed by immunoblotting using three

different titin-antibodies (Figure 1A and 1D). The molecular weight of the N2B-isoform was indistinguishable between normal and DCM-HH tissue and compared well with that of adult rat and pig heart (Figure 1B). In contrast, N2BA-titin expression differed among LV-samples. DCM HH expressed a broader N2BA-band and relatively more N2BA-isoform than control-HH (Figure 1B and 1C). The N2BA-isoforms of HH-tissue were within the size range of rat and adult pig cardiac N2BA-isoforms, which appeared as doublet bands (Figure 1B), and were similar in size and appearance to neonatal pig-cardiac N2BA-isoforms, which migrated as a fuzzy band (Figure 1C). Because truncated titin (MW  $\approx$  1.1 to 2.0 MDa) has been reported to be present in skeletal muscles of patients with familial forms of DCM attributable to titin mutations<sup>7</sup> and in failing HH-tissue,<sup>25</sup> we analyzed all normal-donor and DCM samples for possible expression of low molecular weight forms of titin. However, no truncated proteins in the reported size range were detectable by immunoblotting with I17 (Figure 1D) or the other titin-antibodies.

### Titin-Binding Protein Obscurin Undergoes Isoform Shifting in Human DCM

Another large sarcomere protein, obscurin,<sup>26</sup> appeared on immunoblots of normal-HHs as a strong but fuzzy band at  $\approx$ 900 kDa (Figure 1D, left arrows) and a less obvious second band of lower molecular weight. In DCM hearts ( $n=4$ ), the lower obscurin band was generally stronger than the upper band (Figure 1D, right arrows), indicating disease-related isoform switching also of this titin-binding protein.

### SDS-PAGE Detects No Transmural Differences in Normal N2BA:N2B Ratios

Although titin expression was usually studied in the anterolateral-midwall region of the free LV-wall, we wanted

to know whether possible changes in the N2BA:N2B ratio from subendocardium to subepicardium<sup>20</sup> might be a potential source of variability in results. Hence, we measured the transmural distribution of the N2BA:N2B ratio (Figure 2A) in normal LV-tissue obtained from a set of nine additional donor-HHs (set2). No statistically significant transmural differences were found (Figure 2A). Mean values ( $\pm$ SD) for the proportion of N2BA-isoform were  $28.6\pm 2.2\%$  (endocardium),  $29.1\pm 2.0\%$  (midwall), and  $28.7\pm 2.2\%$  (epicardium).

### DCM Hearts Show Increased N2BA:N2B Titin-Isoform Ratios

Results summarizing the N2BA:N2B titin-protein ratios in controls and DCM hearts are shown in Figure 2B through 2E. Because multiple tissue samples were solubilized and analyzed per heart, we first calculated the mean proportion of N2BA-titin (N2BA+N2B=100%) in individual hearts (Figure 2B) and then determined the “mean of means” for each HH-group (Figure 2C). The proportion of N2BA-titin in DCM hearts,  $42.0\pm 6.1\%$  (mean $\pm$ SD; n=9), was significantly higher ( $P<0.001$ , Student *t* test) than that in set1-donor hearts ( $32.1\pm 2.2\%$ ; n=10) (Figure 2C) or set2-donors (see earlier). Figure 2E groups the relative N2BA-content of individual hearts in five-percentage bins. The 19 donor HHs analyzed (mid-wall region) showed a relatively narrow distribution (range,  $\approx 25\%$  to  $35\%$  N2BA) with a mean $\pm$ SD of  $30.7\pm 2.6\%$ . In contrast, the proportion of N2BA-titin was increased by various degrees in almost all DCM hearts (range,  $\approx 35\%$  to  $55\%$ ) and was similar to that found previously in end-stage failing human ischemic CAD-hearts<sup>19</sup> (Figure 2E).

The total-titin content (N2B+N2BA) per unit tissue was not different between normal and DCM samples (Figure 2D). Although the average content was lower by  $\approx 13\%$  in DCM, the change did not reach statistical significance. However, some DCM hearts showed a clearly reduced total-titin content; then, the loss affected N2BA and N2B isoforms to a similar degree (data not shown). Regression analyses indicated no correlation ( $P\gg 0.05$ ) between the total-titin content of individual HHs and the N2BA:N2B-expression ratio, for both set1-donors and DCM hearts.

### Upregulation of Long, Compliant N2BA-Titin Isoforms in DCM

On gels loaded with similar amounts of titin-protein (gels were handled in an identical manner), the broadness of N2B and N2BA bands was measured in set1-controls and DCM samples by determining the full-width at half-maximum peak heights (FWHM) in intensity profiles (Figure 3A). Whereas the FWHM of the N2B-signal was the same in both HH-groups, that of the N2BA-signal was significantly broader, on average by 48%, in DCM relative to normal-HH tissue (Figure 3B). The histograms in Figure 3B (inset) demonstrate the N2BA-FWHM-values of individual hearts. Further, the N2B-peak position was unaltered in failing versus normal HH, but the distance between the N2BA and N2B peaks was increased in a statistically significant manner in DCM (Figure 3B). Thus, DCM tissue has a larger variety of N2BA-titin isoforms expressed. Especially the N2BA-titins of highest

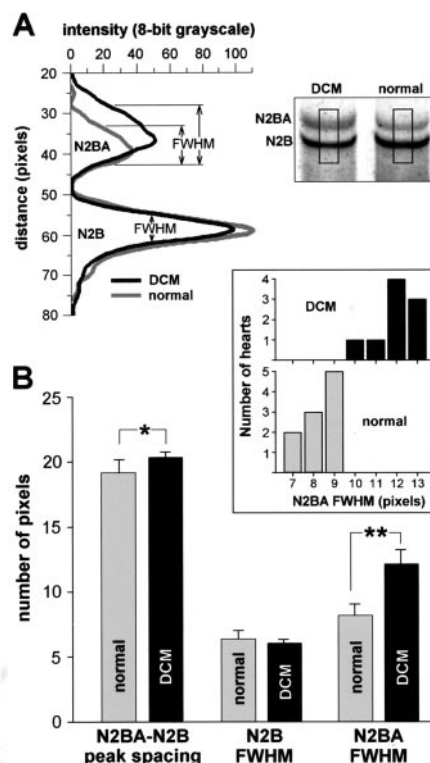


**Figure 3.** Increased expression of high molecular-weight N2BA-titin isoforms in DCM. A, Intensity profiles of titin bands on 2% SDS-polyacrylamide gels. FWHM indicates full width at half-maximum peak height. B, Average FWHM-values for N2BA and N2B titin bands and average distance between N2BA and N2B peaks; summarized data for 10 normal (set1) and 9 DCM hearts (mean $\pm$ SD). \*\* $P<0.001$ , \* $P<0.05$  (Student *t* test). Inset, histogram distribution of N2BA-FWHM-values.

molecular weight ( $>3.3$  MDa; see Figure 6C) are present in greater amounts than in control-HH.

### At mRNA Level no N2BA:N2B Shift Occurs in DCM, but Total-Titin Transcripts Decrease

The mRNA-levels of total-titin and specific titin-splice variants in six normal-donor hearts and six DCM HHs were measured by quantitative real-time RT-PCR using the DNA-binding dye SYBR-Green. The primer positions chosen are indicated in Figure 4A. The expression of total-titin mRNA was significantly reduced, on average by 47%, in DCM compared with controls (Figure 4B). All titin-splice variants were analyzed relative to total-titin mRNA (Figure 4C; the amount of total-titin-mRNA equals one). The average relative mRNA-amount of all N2BA-variants did not differ significantly between normal and DCM, 113% versus 114% (Figure 4C). Because of some differences in primer efficiency, N2BA-mRNA levels generally seemed slightly higher than total-titin mRNA levels (Figure 4C, Ex107–108). After correction for primer efficiency, N2BA-mRNA mostly constituted between  $\approx 93\%$  and  $98\%$  of total-titin mRNA in both HH-groups (data not shown). N2B-mRNA levels were also not significantly altered, constituting  $\approx 36\%$  in controls and  $\approx 41\%$  in DCM (Figure 4C). Thus, the N2BA:N2B mRNA-ratio remained unchanged in DCM hearts.

In addition, mRNA-expression was measured for four individual N2BA-splice variants. As upregulation of fetal

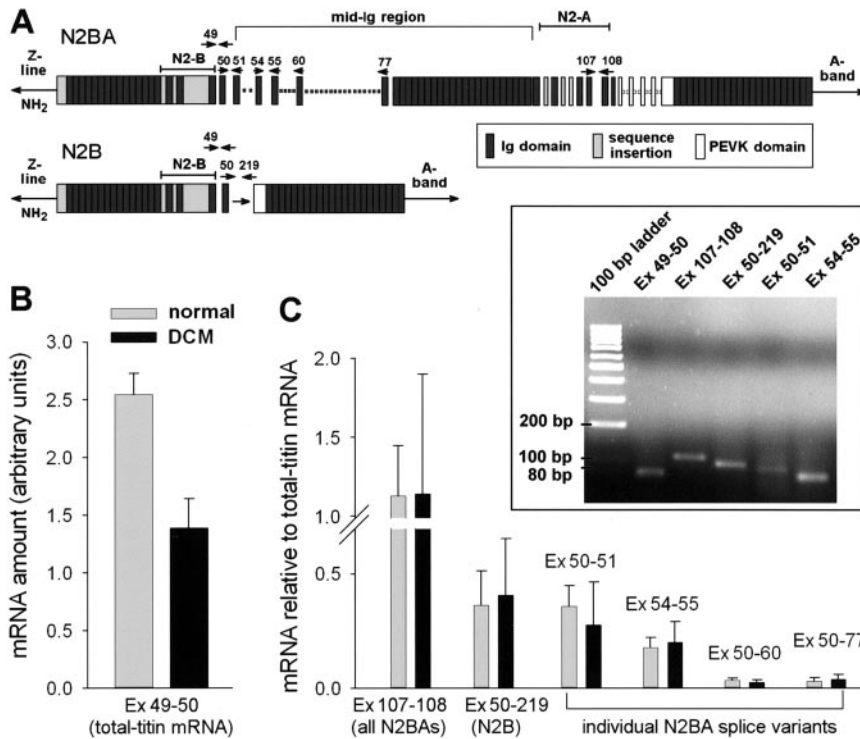


**Figure 4.** Quantification of titin mRNAs in HH-tissue by qRT-PCR. A, Positions of primers used for qRT-PCR (small arrows). Numbers indicate exons in titin's genomic sequence. Inset, Agarose-gel electrophoresis (2%) showing that the primers amplified a single product of the predicted length. Ex indicates exon. B, Average amount of total-titin mRNA in normal-donors and DCM hearts. C, Average amount of all-N2BA, N2B, and individual-N2BA splice-variants relative to total-titin mRNA (the amount of total-titin mRNA equals 1). Data in B and C are mean  $\pm$  SD; DCM, n=6; normal, n=6.

genes is often observed in heart disease, we chose primer-pairs amplifying products suggested to be specific to either adult (exons50–51, exons50–77)<sup>18</sup> or fetal (exons54–55, exons50–60) human titins.<sup>27</sup> Surprisingly, the “fetal” exons were detectable in adult-HH (normal and DCM). Primers to exons54–55 amplified a product constituting (relative to total titin) 18% in controls and 20% in DCM hearts (Figure 4C). The product amplified with primers to exons50–60 amounted to 3.4% in control-donors and 2.4% in DCM. “Adult” splice-variants containing exons50–51 made up  $\approx$ 36% (normal) and 28% (DCM) of total-titin mRNA and those containing exon50 spliced to exon77 made up 3% (normal) and 4% (DCM). With none of the individual-N2BA primer-pairs was a statistically significant difference (Student *t* test) observable between DCM and controls (Figure 4C). Considering that total-titin transcripts were decreased by 47% in DCM, and because all other titin-mRNAs were related to total-titin mRNA, the expression of all analyzed titin-splice variants is downregulated by approximately half in DCM compared with control-donors.

### Myocyte Area Is Decreased in End-Stage Failing DCM Tissue

A possible reason for the decrease in total-titin mRNA in DCM hearts is loss of cardiomyocytes. To test for this possibility, we prepared tissue sections from 7 DCM and 4 normal HHs and used Mallory staining to distinguish cardiomyocytes from connective tissue (Figure 5). Analysis of images (19 from DCM HH; 8 from controls) similar to those shown in Figure 5A revealed a statistically significant decrease in myocyte area ( $P < 0.001$  in Student *t* test) from  $80.9 \pm 12.5\%$  (mean  $\pm$  SD) in normal-HHs to  $53.6 \pm 10.6\%$  in DCM (Figure 5B). Broader and more intense areas of

blue-color stain on DCM sections were indicative of increased collagenous connective tissue.

### Titin-Based Passive Stiffness Is Reduced in Human DCM

Force measurements were performed on nonactivated cardiac myofibrils (Figure 6) obtained from four normal-donor HHs and four failing DCM hearts. All myofibrils included in the analysis (n=10, for each HH-group) presented a regular sarcomere pattern (Figure 6B, inset) and their slack SL in relaxing buffer was  $\approx 1.85 \mu\text{m}$ . Force was measured during 1-second stretch, followed by 19-second hold, protocols and peak, decaying (viscous/viscoelastic), and elastic PT-components were recorded during each step as shown in Figure 6A. Some myofibrils were immunostained with titin-antibody MG1 following the force recordings, to check for (ir)regularity of N2BA-isoform expression in the particular preparations used for mechanical investigation. As in the example of Figure 6B (inset), all myofibrils analyzed by immunofluorescence microscopy showed a regular cross-striated staining pattern; no obvious differences were detectable among controls and DCM samples. Averaged force-extension data revealed a statistically significant depression of peak (elastic+viscous) and elastic-only PT-components in DCM cardiomyofibrils, in the SL-range 2.0 to 2.4  $\mu\text{m}$  (Figure 6B). In contrast, the decaying PT-component (viscous forces only) was not different between controls and DCM myofibrils. The mean reduction of both total (peak) and elastic tension in DCM samples amounted to 23% to 28% at all SLs  $\geq 2.0 \mu\text{m}$ , indicating that the difference between the HH-groups was due mainly to the elastic, titin-derived, PT-component.

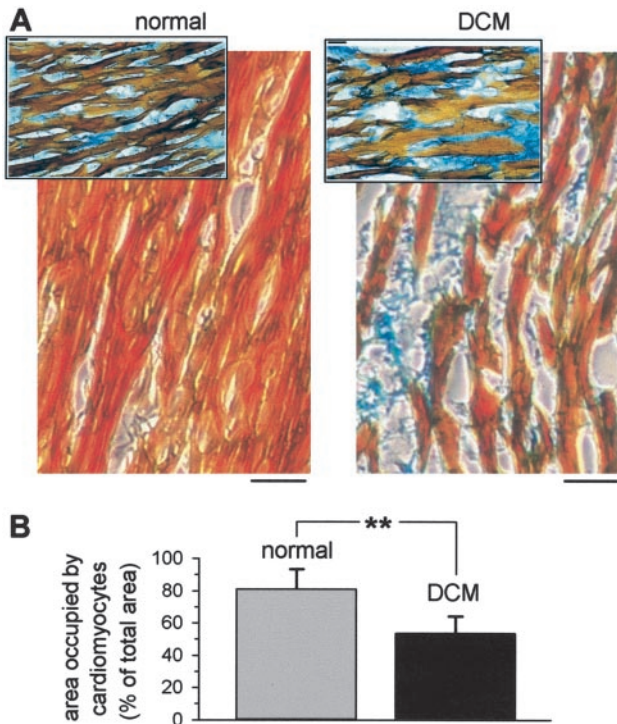


**Figure 5.** Loss of myocytes and increased fibrosis in DCM. A, Sections of normal-donors and DCM HHs stained with Mallory trichrome to distinguish cardiomyocytes (brown-orange) and connective tissue (blue). Bars=40  $\mu$ m. B, Area occupied by cardiomyocytes relative to total area. DCM HHs, n=7 (19 sections); normal-HHs, n=4 (8 sections). \*\* $P$ <0.001 (Student  $t$  test)

### Elastic Myofibrillar PT Is Predictable From the Molecular Weight of Titin-Isoforms

We wanted to know whether the magnitude of PT-decrease measured in DCM myofibrils correlates with the magnitude expected from the titin-isoform shift. Therefore, the results of the gel-electrophoretic analysis were used to predict titin-derived PT. First we tried to emulate the intensity profiles for titin-bands on “typical” gel lanes—those lanes showing N2BA and N2B expression patterns comparable to the average situation—by Gaussian fitting routines (Figure 6C, insets). The N2B-peak was well reproduced by a single Gaussian, whereas the N2BA-peak required fitting with a two-Gaussian. Indeed, separation of the human cardiac N2BA-titin signal into two fuzzy peaks was evident on some gels (data not shown). In representative fits (Figure 6C, insets), the estimated molecular weights of titin-isoforms,  $\approx$ 3 MDa for N2B and  $\approx$ 3.2 to 3.35 MDa for N2BA, were consistent with those suggested by sequencing.<sup>18</sup> In some DCM hearts, the estimated size of N2BA-isoforms reached up to  $\approx$ 3.5 MDa.

The elastic force of titin was modeled as that of three independent worm-like chains corresponding to titin’s tandem-Ig regions, the PEVK-domain, and the N2-B-unique sequence.<sup>11</sup> The prediction used the human titin-sequence information<sup>18</sup> and mechanical parameters of cardiac titin-domain function established by single-molecule force-spectroscopy<sup>11</sup> (see online data supplement). The contributions of the three worm-like chains to total titin force were weighted in proportion to the relative areas under each

individual Gaussian fit. Measured PT-data could be reproduced best with the calculated single-molecule force-data being multiplied by a scaling factor of  $2.2 \times 10^9$  titin molecules per  $\text{mm}^2$  (Figure 6C), very near the cross-sectional packing density of titin in the myofibril ( $2.4 \times 10^9$  molecules/ $\text{mm}^2$ ).<sup>28</sup> The results confirmed that the titin-isoform shift in DCM HH reduces titin-based PT by  $\approx$ 25% to 30% (Figure 6C).

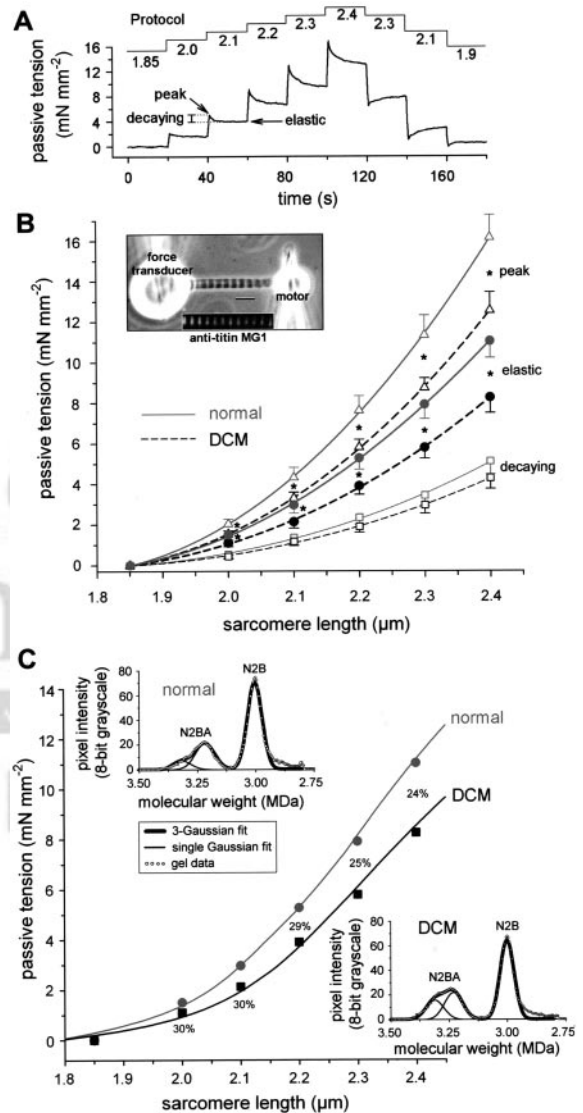


**Figure 6.** Passive-force measurements on isolated human cardiomyofibrils. A, Stretch protocol (top; with SL ( $\mu$ m) indicated) and measured PT. B, Summary of results of PT-recordings on normal and DCM cardiomyofibrils. Peak, PT at end of 1-second stretch; elastic, PT after 19 seconds of stress-relaxation; decaying, viscous/viscoelastic PT-component. Data are mean  $\pm$  SEM; n=10. \* $P$ <0.05 in Student  $t$  test. Inset, Phase-image of human cardiomyofibril and immunofluorescence image after staining with MG1-antibody to N2BA-titin and Cy3-conjugated secondary antibody. Bar=5  $\mu$ m. C, Modeling titin-based (elastic) tension (curves) based on the titin-isoform composition in normal and DCM HH-myofibrils and using the worm-like chain model of entropic elasticity.<sup>11</sup> Data points are from B, “elastic.” Percentage-values indicate predicted PT-reduction in DCM. Insets, intensity of titin-bands on 2% SDS-polyacrylamide gels fitted by Gaussian curves.

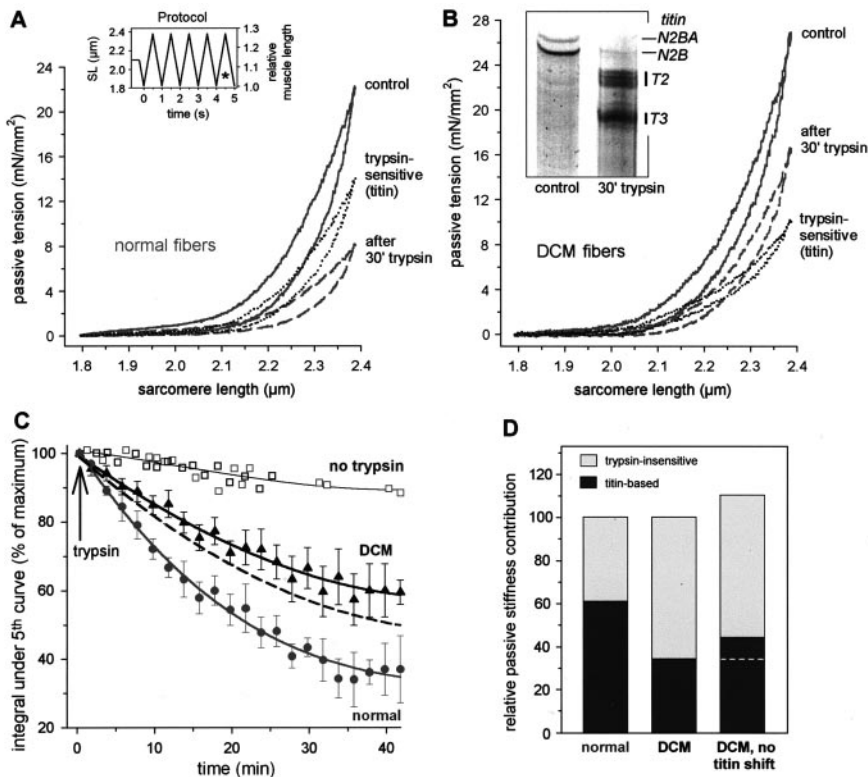


**Figure 7.** Passive tension of skinned HH-fiber bundles during 1-Hz stretch-release cycles, before and after proteolysis of titin. A, PT of normal HH-fiber bundle measured before (solid curve) and after 30-minute long treatment with 0.25  $\mu\text{g}/\text{mL}$  trypsin (dashed curve). Trypsin-sensitive PT indicates titin-based tension (dotted curve). Inset: stretch protocol (asterisk denotes 5th cycle, from which PT is shown). B, PT during the 5th stretch-release cycle as in A, but measured on DCM-HH-fiber bundle. Inset, trypsin-induced titin-degradation detected by 2% SDS-PAGE (T2+T3, degradation products). C, Summary data, the area under the 5th stretch-release curve was determined at 2-minute intervals and is shown relative to the area at time 0. Normal-HH fibers, circles;  $n=15$  (3 hearts). DCM fibers, triangles;  $n=10$  (3 hearts). Data are mean  $\pm$  SEM. Normal or DCM fibers not treated with trypsin, gray and black squares, respectively;  $n=2$  each. Fits are third-order regressions. Dashed line is DCM curve if there were no titin-isoform shift. D, Relative contribution of titin, compared with that of trypsin-insensitive structures, to total passive myocardial stiffness. Data are estimated from the fits in the main figure at time-point 40 minutes.

### Proportion of Titin-Based Passive Stiffness Is Reduced in DCM

To understand the role of titin-isoform switching for the global passive stiffness of human DCM hearts, we performed mechanics on nonactivated HH-fiber bundles. Five 1-Hz cycles covering a SL-range of 1.8 to  $\approx 2.4$   $\mu\text{m}$  (Figure 7A, inset) were applied to chemically skinned HH-fiber bundles every  $\approx 2$  minutes, and PT in the 5th loop was analyzed before and after exposure of the samples to 0.25  $\mu\text{g}/\text{mL}$  trypsin (Figure 7A,B).<sup>24</sup> Low doses of trypsin degrade titin selectively.<sup>24,29</sup> In our hands, intact titin visualized by 2% SDS-PAGE decreased to barely detectable levels within 30 to 40 minutes of trypsin treatment (Figure 7B, inset). Titin proteolysis depressed the PT of HH-fiber bundles, but the reduction was much greater in normal than in DCM-HH tissue (Figure 7A and 7B). A summary plot showing the area under the 5th stretch-release curve as a measure of passive stiffness (Figure 7C) indicates a steady drop in stiffness with time, until the decrease stops 35 to 40 minutes after application of trypsin, once titin is degraded. The remaining stiffness at 40 minutes is most likely attributable to stiff structures of the cytoskeleton (intermediate filaments) and the ECM (collagen).<sup>24,30</sup> This trypsin-insensitive stiffness was  $\approx 40\%$  (control donors) and  $\approx 65\%$  (DCM samples) the reference stiffness of nontrypsinized normal or DCM-HH fibers at 40 minutes (Figure 7C, fits). Hence, titin-based stiffness made up 60% of total passive stiffness in donor-hearts but only 35% in DCM hearts (Figure 7D). If there were no titin-isoform shift in DCM-HH- and titin-based stiffness thus were higher by approximately 30% (Figure 7C, dashed curve), total passive stiffness would be greater than the measured value, by  $\approx 10\%$ , as there would be a 10% larger contribution

of titin to total stiffness (Figure 7D, right column). These findings indicate that the lower-than-normal relative contribution of titin to total passive stiffness in failing DCM hearts results to some degree from titin-isoform switching but must have other sources as well, probably loss of myocytes and increased fibrosis.

### Discussion

This study highlights the important role of titin for the passive stiffness of human myocardium: end-stage failing hearts of idiopathic-DCM patients were shown to increase the expression of compliant, high-molecular-weight, titin-isoforms, thus reducing titin-based PT. Myocardial PT is determined only in part by titin filaments, but also by ECM material,<sup>10,24,30</sup> and upregulated collagen expression, as well as increased cross-linking of collagen fibers,<sup>30</sup> were suggested to contribute to increased passive stiffness in end-stage failing hearts.<sup>2,5</sup> Other evidence included altered distribution and loss of titin in chronically diseased myocardium of human,<sup>2</sup> hamster,<sup>15</sup> and guinea-pig.<sup>17</sup> Failing human DCM hearts showed remodeling of the ECM and upregulation and disorganization of many cytoskeletal proteins, along with a decrease in titin-protein accompanying a loss of myocytes.<sup>2</sup> Human DCM hearts were also found to have higher-than-normal passive stiffness.<sup>31</sup> In the present work, the relationship between titin-derived passive stiffness and non-titin-based stiffness (ECM, intermediate filaments) was found to be altered in nonischemic DCM HHs: the relative contribution of titin to total passive stiffness was greatly reduced compared with that in control-donor HHs.

Two recent studies suggested that failing human<sup>19</sup> and dog<sup>21</sup> hearts adjust their passive stiffness by titin-isoform switching. Consistent with this proposal, the human DCM

hearts investigated in this study showed a  $\approx 63\%$  increase in the average N2BA:N2B ratio over control-donor HHs (0.72 versus 0.45). This titin-isoform shift is of similar magnitude, and goes in the same direction, as that found in human patients with chronic CAD.<sup>19</sup> We also studied<sup>19</sup> four nonischemic transplant-HHs (two were included in this study, as they had DCM, the others were omitted because of obscure etiology) and reported near-normal proportions of N2BA-titin, but the current analysis of a larger subset of human DCM hearts clearly establishes a significantly increased average N2BA:N2B ratio also in nonischemic HH-disease. The titin-isoform shift found in this study is larger, and goes in the opposite direction, compared with that observed in a 4-week pacing-induced canine DCM model.<sup>21</sup> Thus, the direction and magnitude of titin-isoform switching could depend on whether the disease is chronic in nature (as in long-term ischemic human or rat hearts<sup>19</sup>) or more short-term (as in the canine rapid-pacing model<sup>20,21</sup>).

Interestingly, our gel-electrophoretic analysis showed a relatively narrow distribution of N2BA:N2B ratios in the 19 control-donor HHs (Figure 2E). This suggests that the isoform-ratio of normal HH (at a given location in the LV wall) may be tightly regulated. In contrast, the ratio was quite variable in failing HHs. Because explanted HHs usually represent a variable cohort, it is not clear whether the variability in titin-isoform ratio is attributable to the heterogeneity of pathology and/or severity of the disease. A possibility is that a higher-than-normal N2BA:N2B titin-protein ratio requires long-term increases in preload, as suggested earlier.<sup>19</sup> It is clear that the increased N2BA:N2B ratio in chronically diseased HHs is a way to reduce passive wall stiffness to some degree, in the subset of DCM hearts studied here, on average by  $\approx 10\%$  (Figure 7D). Our results suggested that an important factor in the reduction of titin-based passive stiffness in DCM is the upregulation mainly of high-molecular-weight N2BA-titins  $>3.3$  MDa; smaller N2BA-isoforms are not significantly altered (Figure 3). The increased proportion of compliant N2BA-titins may help preserve the diastolic function of failing myocardium for a longer period of time than possible without the titin-isoform shift.

An issue was the possibility of gradients of titin-isoform ratios across the free LV wall,<sup>20</sup> but such gradients were not found in control-donor HH (Figure 2A). Similarly, normal goat and rabbit hearts showed only minor transmural differences.<sup>32</sup> Then, the transmural-ratio differences found in 2-week-paced dog hearts<sup>20</sup> could represent a specific property of that disease model. Some indirect evidence for the absence of significant transmural differences in diseased human myocardium comes from the observation that PT at  $2.2 \mu\text{m}$  SL is similar in skinned fibers obtained from subendocardial ( $3.5 \pm 0.7$  mN/mm<sup>2</sup>) and subepicardial ( $3.7 \pm 0.6$  mN/mm<sup>2</sup>) human-LV biopsies.<sup>33</sup> However, additional investigation of this issue is needed, also taking into account the existence of gradients in N2BA:N2B ratio from the heart's basis to apex.<sup>32</sup>

Titin-transcript expression was studied previously in a guinea-pig model of hypertrophic cardiomyopathy, demonstrating increased titin-mRNA transcripts in compensated

hypertrophy but declining mRNA-levels in the transition to decompensated CHF.<sup>16</sup> However, information on titin-transcript levels in human-heart disease was lacking. By qRT-PCR, we found that the total-titin-transcript expression was down by approximately half in human-DCM tissue (Figure 4), due mainly to loss of myocytes (Figure 5). Considering the plethora of titin-splice variants in human heart,<sup>18</sup> we also compared the expression levels of various titin-mRNA species in normal and DCM HH. Unlike the titin-isoform ratios, the N2BA:N2B-mRNA ratios were not significantly altered in DCM, and no disease-related changes appeared in the relative amount of individual-N2BA splice variants. These findings suggest that the upregulation of giant-size N2BA-isoforms must occur at a level downstream of alternative splicing—consistent with our conclusion on the regulation of titin-isoform expression during perinatal heart development.<sup>22</sup> Interestingly, we found that human-titin exons previously described as “fetal-specific” by microarray analysis<sup>27</sup> were expressed in both normal and DCM adult-HH. A possible explanation for this discrepancy is the higher sensitivity of the qRT-PCR method for detecting transcripts. In any case, and although more splice-pathways should be studied before a final conclusion can be made, our results do not confirm our initial hypothesis that end-stage failing HH may show increased expression of fetal cardiac-titin splice-pathways. Instead, adult titin-splice variants may be upregulated in DCM.

Force measurements on isolated HH-myofibrils and modeling studies revealed a decrease in titin-based stiffness of end-stage failing DCM HH, on average by  $\approx 25\%$  to  $30\%$  (Figure 6). Skinned-fiber mechanics showed a reduced proportion of titin-derived passive stiffness in DCM (Figure 7), which was not explainable only by titin-isoform shift and upregulation of giant-size N2BA-titins. Other important factors are a reduction in myocyte area and increased connective tissue in DCM (Figure 5), suggesting loss of titin-protein. Because other sarcomere proteins will be lost as well, a measure of the total-titin content could not be obtained from the titin:myosin heavy-chain ratio, as done by others.<sup>21,25</sup> Among the HHs analyzed in this study, the variability in total titin-protein content measured by SDS-PAGE was high and the average reduction in the DCM group, relative to the normal-HH group (13%), was not statistically significant. Sample heterogeneity, but particularly the inherent limits of the gel-detection method,<sup>28</sup> may contribute to difficulties in uncovering changes in total titin-protein content. Taken together, our results suggest that both titin-isoform switching and replacement of myocytes by collagenous connective tissue impact the global passive stiffness of the failing human heart.

The decrease in titin-based passive stiffness, which lowered global stiffness by  $\approx 10\%$ , may benefit myocardial diastolic function. In turn, however, a lowered spring force of titin may have adverse effects on the Frank-Starling mechanism<sup>12,29</sup> and cardiac shortening velocity,<sup>13</sup> and may compromise the mechanical function of the stress-sensing machinery.<sup>14</sup> If so, the titin-isoform switch in failing HH might contribute to systolic dysfunction. Finally, our observation that the titin-binding protein obscurin also undergoes



isoform-switching in human DCM may hint at an intricate web of “players” of the sarcomeric cytoskeleton possibly affected in a coordinated fashion during the remodeling in HH-disease.

### Acknowledgments

We acknowledge support of the Deutsche Forschungsgemeinschaft (Li690/2–3). We thank Dr Vladimir Bene for help with RT-PCR and Antita Kühner and Rudolf Dussel for technical assistance.

### References

- Seidman JG, Seidman C. The genetic basis for cardiomyopathy: from mutation identification to mechanistic paradigms. *Cell*. 2001;104:557–567.
- Hein S, Kostin S, Heling A, Maeno Y, Schaper J. The role of the cytoskeleton in heart failure. *Cardiovasc Res*. 2000;45:273–278.
- Heling A, Zimmermann R, Kostin S, Maeno Y, Hein S, Devaux B, Bauer E, Klovekorn WP, Schlepper M, Schaper W, Schaper J. Increased expression of cytoskeletal, linkage, and extracellular proteins in failing human myocardium. *Circ Res*. 2000;86:846–853.
- Chien KR, Olson EN. Converging pathways and principles in heart development and disease: CV@CSH. *Cell*. 2002;110:153–162.
- Schaper J, Froede R, Hein S, Buck A, Hashizume H, Speiser B, Friedl A, Bleese N. Impairment of the myocardial ultrastructure and changes of the cytoskeleton in dilated cardiomyopathy. *Circulation*. 1991;83:504–514.
- Itoh-Satoh M, Hayashi T, Nishi H, Koga Y, Arimura T, Koyanagi T, Takahashi M, Hohda S, Ueda K, Nouchi T, Hiroe M, Marumo F, Imaizumi T, Yasunami M, Kimura A. Titin mutations as the molecular basis for dilated cardiomyopathy. *Biochem Biophys Res Commun*. 2002;291:385–393.
- Gerull B, Gramlich M, Atherton J, McNabb M, Trombitas K, Sasse-Klaassen S, Seidman JG, Seidman C, Granzier H, Labeit S, Frenneaux M, Thierfelder L. Mutations of TTN, encoding the giant muscle filament titin, cause familial dilated cardiomyopathy. *Nat Genet*. 2002;30:201–204.
- Xu X, Meiler SE, Zhong TP, Mohideen M, Crossley DA, Burggren WW, Fishman MC. Cardiomyopathy in zebrafish because of mutation in an alternatively spliced exon of titin. *Nat Genet*. 2002;30:205–209.
- Miller MK, Granzier H, Ehler E, Gregorio CC. The sensitive giant: the role of titin-based stretch sensing complexes in the heart. *Trends Cell Biol*. 2004;14:119–126.
- Linke WA, Fernandez JM. Cardiac titin: molecular basis of elasticity and cellular contribution to elastic and viscous stiffness components in myocardium. *J Muscle Res Cell Motil*. 2002;23:483–497.
- Li H, Linke WA, Oberhauser AF, Carrion-Vazquez M, Kerkvliet JG, Lu H, Marszalek PE, Fernandez JM. Reverse engineering of the giant muscle protein titin. *Nature*. 2002;418:998–1002.
- Granzier H, Labeit S. Cardiac titin: an adjustable multi-functional spring. *J Physiol*. 2002;541:335–342.
- Opitz CA, Kulke M, Leake MC, Neagoe, Hinssen H, Hajjar RJ, Linke WA. Damped elastic recoil of the titin spring in myofibrils of human myocardium. *Proc Natl Acad Sci U S A*. 2003;100:12688–12693.
- Knoll R, Hoshijima M, Hoffman HM, Person V, Lorenzen-Schmidt I, Bang ML, Hayashi T, Shiga N, Yasukawa H, Schaper W, et al. The cardiac mechanical stretch sensor machinery involves a Z-disc complex that is defective in a subset of human dilated cardiomyopathy. *Cell*. 2002;111:943–955.
- Kawaguchi N, Fujitani N, Schaper J, Onishi S. Pathological changes of myocardial cytoskeleton in cardiomyopathic hamster. *Mol Cell Biochem*. 1995;144:75–79.
- Collins JF, Pawloski-Dahm C, Davis MG, Ball N, Dorn GW 2nd, Walsh RA. The role of the cytoskeleton in left ventricular pressure overload hypertrophy and failure. *J Mol Cell Cardiol*. 1996;28:1435–1443.
- Wang X, Li F, Campbell SE, Gerdes AM. Chronic pressure overload cardiac hypertrophy and failure in guinea pigs: II. Cytoskeletal remodeling. *J Mol Cell Cardiol*. 1999;31:319–331.
- Freiburg A, Trombitas K, Hell W, Cazorla O, Fougousse F, Centner T, Kolmerer B, Witt C, Beckmann JS, Gregorio CC, Granzier H, Labeit S. Series of exon-skipping events in the elastic spring region of titin as the structural basis for myofibrillar elastic diversity. *Circ Res*. 2000;86:1114–1121.
- Neagoe C, Kulke M, del Monte F, Gwathmey JK, de Tombe PP, Hajjar RJ, Linke WA. Titin isoform switch in ischemic human heart disease. *Circulation*. 2002;106:1333–1341.
- Bell SP, Nyland L, Tischler MD, McNabb M, Granzier H, LeWinter MM. Alterations in the determinants of diastolic suction during pacing tachycardia. *Circ Res*. 2000;87:235–240.
- Wu Y, Bell SP, Trombitas K, Witt CC, Labeit S, LeWinter MM, Granzier H. Changes in titin isoform expression in pacing-induced cardiac failure give rise to increased passive muscle stiffness. *Circulation*. 2002;106:1384–1389.
- Opitz CA, Leake MC, Makarenko I, Benes V, Linke WA. Developmentally regulated switching of titin size alters myofibrillar stiffness in the perinatal heart. *Circ Res*. 2004;94:967–975.
- Kulke M, Fujita-Becker S, Rostkova E, Neagoe C, Labeit D, Manstein DJ, Gautel M, Linke WA. Interaction between PEVK-titin and actin filaments: origin of a viscous force component in cardiac myofibrils. *Circ Res*. 2001;89:874–881.
- Wu Y, Cazorla O, Labeit D, Labeit S, Granzier H. Changes in titin and collagen underlie diastolic stiffness diversity of cardiac muscle. *J Mol Cell Cardiol*. 2000;32:2151–2162.
- Morano I, Hadicke K, Grom S, Koch A, Schwinger RH, Bohm M, Bartel S, Erdmann E, Krause EG. Titin, myosin light chains and C-protein in the developing and failing human heart. *J Mol Cell Cardiol*. 1994;26:361–368.
- Young P, Ehler E, Gautel M. Obscurin, a giant sarcomeric Rho guanine nucleotide exchange factor protein involved in sarcomere assembly. *J Cell Biol*. 2002;154:123–136.
- Lahmers S, Wu Y, Call DR, Labeit S, Granzier H. Developmental control of titin isoform expression and passive stiffness in fetal and neonatal myocardium. *Circ Res*. 2004;94:505–513.
- Liversage AD, Holmes D, Knight PJ, Tskhovrebova L, Trinick J. Titin and the sarcomere symmetry paradox. *J Mol Biol*. 2001;305:401–409.
- Helmes M, Lim CC, Liao R, Bharti A, Cui L, Sawyer DB. Titin determines the Frank-Starling relation in early diastole. *J Gen Physiol*. 2003;121:97–110.
- Burlew BS, Weber KT. Cardiac fibrosis as a cause of diastolic dysfunction. *Herz*. 2002;27:92–98.
- Vahl CF, Timek T, Bonz A, Kochsiek N, Fuchs H, Schaffer L, Rosenberg M, Dillmann R, Hagl S. Myocardial length-force relationship in end stage dilated cardiomyopathy and normal human myocardium: analysis of intact and skinned left ventricular trabeculae obtained during 11 heart transplantations. *Basic Res Cardiol*. 1997;92:261–270.
- Neagoe C, Opitz CA, Makarenko I, Linke WA. Gigantic variety: expression patterns of titin isoforms in striated muscles and consequences for myofibrillar passive stiffness. *J Muscle Res Cell Motil*. 2003;24:175–189.
- van der Velden J, Klein LJ, van der Bijl M, Huybregts MA, Stooker W, Witkop J, Eijnsman L, Visser CA, Visser FC, Stienen GJ. Isometric tension development and its calcium sensitivity in skinned myocyte-sized preparations from different regions of the human heart. *Cardiovasc Res*. 1999;42:706–719.